Physica Scripta. Vol. T115, 705–708, 2005

Ni K- and Au L_3-edge XAFS of $[Au_6Ni_{32}(CO)_{44}]^{6-}$ and a Study of its Transformations in Acetonitrile Solutions

O. A. Belyakova[1,*], Y. Kubozono[2], S. Kashino[2] and Yu. L. Slovokhotov[1]

[1]Nesmeyanov Institute of Organoelement compounds, RAS, 28 Vavilov St., Moscow 119991, Russia
[2]Department of Chemistry, Okayama University, Okayama 700-8530, Japan

Received June 26, 2003; accepted November 4, 2003

PACS numbers: 81.07.−b, 61.10.Ht

Abstract

Oxidation of the $[Au_6Ni_{32}(CO)_{44}]^{6-}$ cluster anion in acetonitrile solutions by air and by Me_3NO has been monitored using Ni K- and Au L_{III}-edge XAFS spectroscopy. EXAFS data for the pristine cluster correspond reasonably well to its known crystal structure and point to a formation of bimetallic Ni-Au nanoparticles in the oxidation products. Air oxidation of the acetonitrile solutions without additional oxidants/promoters goes very slowly whereas addition of Me_3NO results in immediate precipitation. The nanoparticles formed upon the oxidation are suggested to have a core of gold atoms and an outer shell of nickel oxide.

1. Introduction

Transition metal nanoparticles have attracted significant attention over the last decade [1–3]. Their potential application areas encompass, among others, catalysis, medicine, and electronics. One of the most promising synthetic approaches to metal nanoparticles is a controlled chemical transformations of well-characterized molecular precursors, *e.g.* high-nuclearity cluster compounds [2]. Up to date, a wealth of stoichiometric cluster compounds with cluster cores ranging from highly ordered fragments of close packings to loose irregular agglomerates are known [3], which can be used as building blocks in a design of new metal-based nanostructured materials. An especially important class of these materials consists of bimetallic nanoparticles, which allow fine tuning of the materials' properties due to a variability of their chemical compositions and spatial distributions of the component metal atoms in cluster cores [4].

Recently, a new high-nuclear stoichiometric bimetallic carbonyl cluster $[Au_6Ni_{32}(CO)_{44}]^{6-}\cdot 6PPh_4\cdot 4.5CH_3CN$ was synthesized, isolated, and characterized by single-crystal X-ray diffraction by L. F. Dahl and his group [5]. According to the crystallographic data, the core of the cluster anion (Fig. 1) is built up of an inner Au_6 octahedron surrounded by a Ni_{32} shell. In the idealized D_{3d} point symmetry of the Au_6Ni_{32} bimetallic moiety, five types of Ni atoms are symmetrically non-equivalent (meanwhile, the crystallographic symmetry of the core is P-1 such that 16 Ni atoms are crystallographically independent). In overall, the structure is characterized by broad distributions of all interatomic contacts. Upon mild heating or chemical oxidation, this cluster readily loose its carbonyl ligands to form higher-nuclearity species. Therefore, it may be a convenient precursor in preparation of bimetallic Ni-Au nanoparticles.

XAFS spectroscopy is an important tool to study chemical transformations, which lead to a formation of nanoclusters, *e.g.* colloid metals [1, 6, 7]. Earlier, the oxidative aggregation of various stoichiometric palladium carbonyl-phosphine clusters exposed to air in toluene solutions, giving rise to f.c.c. Pd_n nanoparticles (where n is *ca*. 900) was monitored by us using Pd K-edge EXAFS and XRD [8].

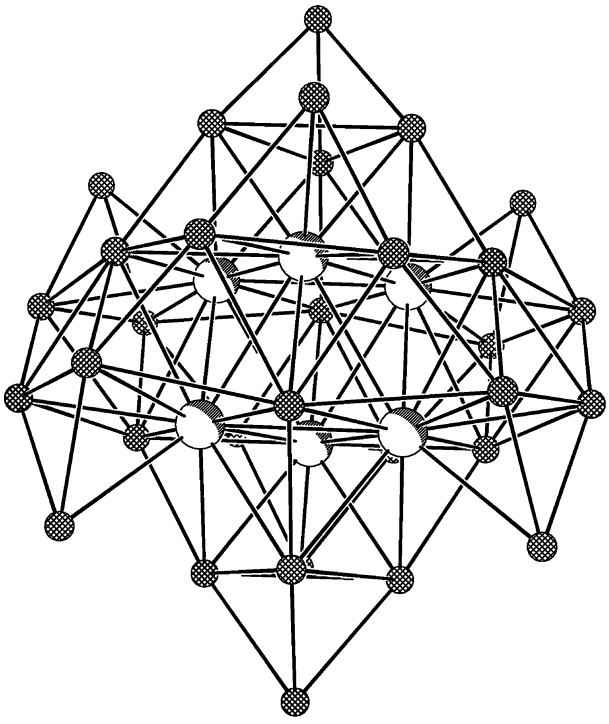

Fig. 1. Cluster core of the initial Au_6Ni_{32} cluster according to the X-ray crystallographic analysis [5]. Large spheres denote Au atoms, small spheres denote Ni atoms.

In this paper, we report on Au L_{III}- and Ni K-edge XAFS monitoring of the evolution of the $[Au_6Ni_{32}(CO)_{44}]^{6-}$ cluster anion in acetonitrile solutions upon oxidation. As it was shown elsewhere [9], Me_3NO readily transfer an oxygen atom to carbonyl ligands to form CO_2 and thus strongly promotes the overall oxidation of transition metal carbonyls in the presence of air. Thus, both oxidation routes with and without the promoter were studied.

2. Experimental

Polycrystalline cluster compound $[Au_6Ni_{32}(CO)_{44}]^{6-}\cdot 6PPh_4\cdot$ 4.5MeCN (hereinafter, referred to as Au_6Ni_{32}; 25 mg) was provided by Prof. Lawrence F. Dahl (University of Wisconsin-Madison, USA). Commercially available acetonitrile was further purified from air by Ar bubbling for 10 min. Two samples of dark brown acetonitrile solutions with a concentration of *ca*. 20 g/l for

*e-mail: obelyak@ineos.ac.ru

the first solution (**1**) and *ca*. 30 g/l for the second solution (**2**) were prepared by ultrasonication (1 min) of the respective amounts of Au_6Ni_{32} in *ca*. 0.5 ml of MeCN. For measurements, *ca*. 0.1 ml of both solutions were placed in small plastic cells, which were open to air. The rest of the two solutions, kept closed from air, maintained brown colour with some brown precipitate formed. In order to promote the oxidation, 3 mg of a mild oxidant Me_3NO (*ca*. 10 : 1 excess with respect to the initial cluster) dissolved in several drops of EtOH/MeOH mixture was added to the fraction of the solution **2** kept in a closed vessel for 10 hours. The brown colour of the solution immediatly disappeared and a brown flake-like precipitate evolved, which was separated afterwards onto a paper filter.

The polycrystalline powder of the initial Au_6Ni_{32} cluster (in Ar-blown polyethylene bags), solutions **1** and **2**, and the resulting precipitate were studied by XAFS in the fluorescence yield mode at the BL-9A bending magnet beamline of the Photon Factory synchrotron facility (KEK, Tsukuba, Japan) operated at 2.5 GeV with the electron current stored of 300 mA. The beam was focused on a sample by a system of conical Rh-coated mirrors to give a spotsize of $0.35 \times 1\,mm^2$. Intensity of the primary beam monocromatized by a Si(111) double crystal monocromator was measured by an ionization chamber filled with nitrogen; X-ray fluorescence yield was measured using a Lyttle detector. XAFS data for the air-exposed solutions **1** and **2** were collected repeatedly every 15–20 minutes (XANES) or 2–2.5 hours (EXAFS) with a total duration of 10 hours. The standard processing of EXAFS spectra was performed using the UWXAFS [10] software package with *ab initio* scattering amplitude and phase functions calculated by FEFF [11]. Normalized EXAFS curves $k^3\chi(k)$ over the k ranges of 2.6–12 $Å^{-1}$ for most of the spectra and 2.6–15 $Å^{-1}$ for the Au L_{III} spectrum of the precipitate were used in the curve-fitting.

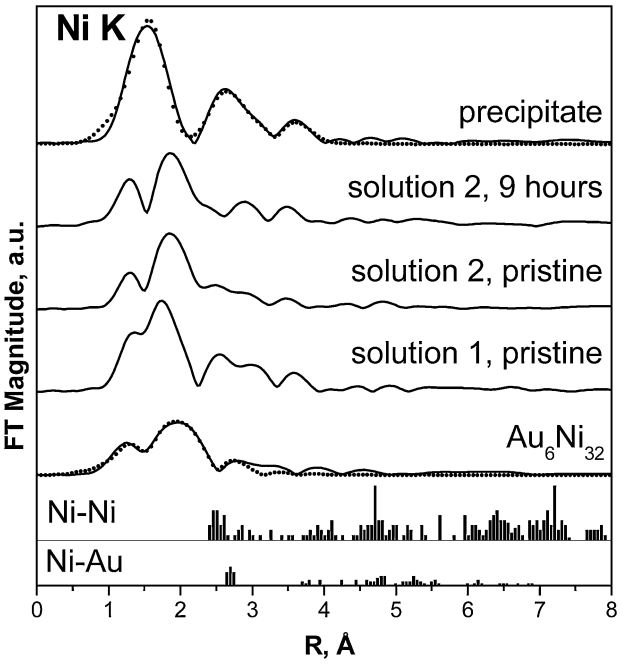

Fig. 2. Fourier transforms of Ni K-edge EXAFS spectra for the initial Au_6Ni_{32} cluster, pristine acetonitrile solutions **1** and **2**, solution **2** exposed to air for 9 hours, and the precipitate: experiment (solid lines) and best-fits (dots). Histograms of Ni-Ni and Ni-Au interatomic distances in the initial Au_6Ni_{32} cluster are shown for comparison.

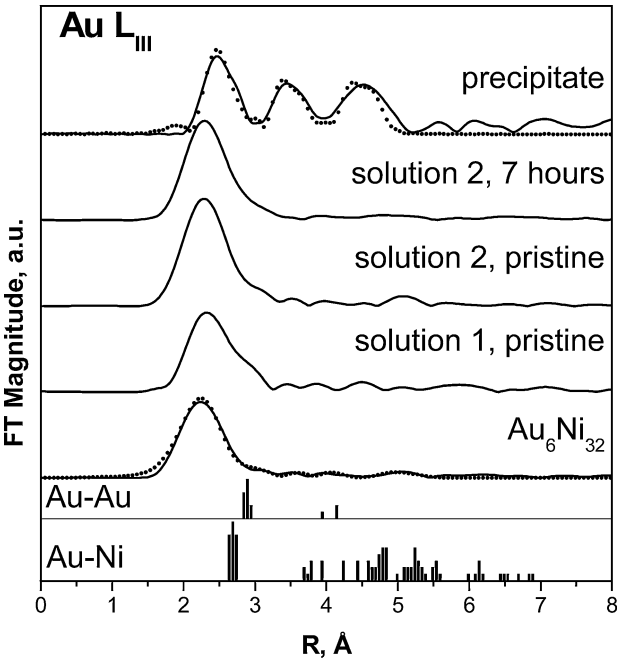

Fig. 3. Fourier transforms of Au L_{III}-edge EXAFS spectra for the initial Au_6Ni_{32} cluster, pristine acetonitrile solutions **1** and **2**, solution **2** exposed to air for 7 hours, and the precipitate: experiment (solid lines) and best-fits (dots). Histograms of Au-Ni and Au-Au interatomic distances in the initial Au_6Ni_{32} cluster are shown for comparison.

3. Results and discussion

Typical Fourier transforms (FTs) of Ni K- and Au L_{III}- edge EXAFS for the studied samples are shown in Figs. 2 and 3, respectively. Best-fit curves for the initial cluster and the resulting precipitate, are shown in dotted lines. Values of structural parameters corresponding to the best-fit structural models are summarized in Table I.

Due to the low symmetry of the Au_6Ni_{32} core in the initial cluster (see histograms of metal-metal distances shown in Figs. 2 and 3), fitting procedure of EXAFS spectra is challenging, especially in the case of Ni K-edge data. Nevertheless, a minimum required model of Au_6Ni_{32} composed of two Ni-C (Ni-C1 and Ni-C2), Ni-Ni, Ni-Au, and Ni . . . O spheres showed a pronounced similarity to the experimental Ni K-edge FT. The obtained best-fit values for the interatomic distances lie within the distribution limits of the respective parameters known from crystallographic data (see Table I). The FT pattern at Au L_{III}-edge even better corresponds to the structural model; its main peak is formed by overlapping contributions from closest Au-Ni and Au-Au distances. The pattern of relatively weak peaks at 3–5 Å can be well fitted to a set of outer spheres including non-bonding Au . . . C as well as Au . . . Ni and Au . . . Au separations in a good agreement with the crystallographic data.

The FTs of the precipitate are drastically different from those of the initial compound indicating a deep rearrangement of both the cluster core and the ligand shell due to the oxidation. The first dominant peak in the Ni K-edge FT can be well simulated with Ni-O scattering path at 2.03 Å that strongly suggests that a substitution of carbonyl ligands by oxygen atoms occurred. The shortest Ni-Ni distance is 2.93 Å according to the fitting results. Both these values are close to corresponding Ni-O and Ni . . . Ni distances in cubic crystalline nickel oxide NiO of NaCl type [12]. At Au L_{III}-edge, the FT is composed of three distinct peaks at *ca*. 2.45 Å, 3.45 Å, and 4.52 Å (not corrected for the phase shift). The high intensities of these peaks

Table I. *Best-fit values of EXAFS structural parameters for the initial Au_6Ni_{32} cluster and the final product of its oxidation by Me_3NO compared to X-ray diffraction data.*

	EXAFS			X-ray diffraction	
Path	R, Å	N	σ^2, Å^2	R/R_{mean}, Å	N_{mean}
Au_6Ni_{32}, Ni K-edge ($R_f = 0.03$)				Au_6Ni_{32} [5]	
Ni-C1	1.90	1.1	0.002	1.75–2.05/1.90	2.7
Ni-C2	2.08	1.6	0.002		
Ni-Ni	2.45	3.0	0.016	2.37–2.60/2.48	3.0
Ni-Au	2.74	1.5	0.007	2.62–2.76/2.68	1.5
Ni…O	2.77	2.7	0.009	2.83–2.94/2.89	2.7
Au_6Ni_{32}, Au L_{III}-edge ($R_f = 0.02$)				Au_6Ni_{32} [5]	
Au-Ni	2.64	8.0	0.014	2.62–2.76/2.68	8.0
Au-Au	2.92	4.0	0.021	2.83–2.94/2.89	4.0
Au…C	3.54	5.0	0.011	3.49–3.70/3.61	5.0
Au…Ni	3.76	3.0	0.020	3.66–3.94/3.79	3.0
Au…Au	4.05	1.0	0.005	3.95–4.15/4.07	1.0
Au…Ni	5.35	2.0	0.009	—	—
Precipitate, Ni K-edge ($R_f = 0.03$)				NiO [12]	
Ni-O	2.03	3.9	0.009	2.09	6
Ni-Au1	2.73	2.1	0.010		
Ni…Ni1	2.93	9.7	0.029	2.95	12
Ni…Au2	3.70	2.6	0.009		
Ni…Ni2	3.84	13.4	0.026	4.18	6
Precipitate, Au L_{III}-edge ($R_f = 0.05$)				Bulk Au [13]	
Au-Ni1	2.75	1.5	0.004		
Au-Au1	2.70	4.0	0.008	2.88	12
Au…Ni2	3.67	2.0	0.002		
Au…Au2	3.59	10.0	0.008	4.08	6
Au…Ni3	4.67	3.8	0.001		
Au…Au3	4.58	16.1	0.006	5.00	24

assume a relatively big cluster core with a well-ordered local environment of gold atoms [13]. According to the fitting results, both gold and nickel contribute to these three peaks with the gold contribution dominating. Furthermore, Ni-Au interatomic distances independently determined from Ni K- and Au L_{III}-edge data (Au-Ni1/Ni-Au1 and Au…Ni2/Ni…Au2 in Table I) are consistent. No fitting-improving Au-A contributions (where A denotes oxygen or other light atoms) were found.

In Ni K-edge XANES (Fig. 4), the pattern of the precipitate with a weak pre-edge feature and an intense main component ("white line"), is totally different from that of the initial cluster compound, which has a strong pre-edge peak and a weak white line. The pre-edge feature, which appears due to a forbidden $1s \rightarrow 3d$ electronic transitions is always prominent for compounds with direct Ni-Ni bonds. A strong reduction of this feature gives an evidence that a substantial part of Ni-Ni bonds was broken as a result of the oxidation in accordance with EXAFS data, where only non-bonding Ni…Ni closest distances are observed.

Therefore, our XAFS data indicate that nanoparticles composed of an Au core and a NiO outer shell are most probably formed upon the chemical oxidation of the initial $[Au_6Ni_{32}(CO)_{44}]^{6-}$ cluster anion with Me_3NO. It has to be mentioned that Au-Au interatomic distances (2.70 Å, 3.59 Å, and 4.58 Å) are significantly shorter than in the bulk f.c.c. gold (2.88 Å, 4.07 Å, and 4.99 Å, respectively) that may point to a different, *viz.* non-f.c.c, arrangement of Au atoms in cores of the Au-Ni nanoparticles. The Au-Au interatomic distances as short as 2.70 Å were also found in high-nuclearity gold cluster compounds by single crystal X-ray diffraction [14].

A comprehensive quantitative analysis of the FT patterns of acetonitrile solutions is too complicated since a lot of scattering

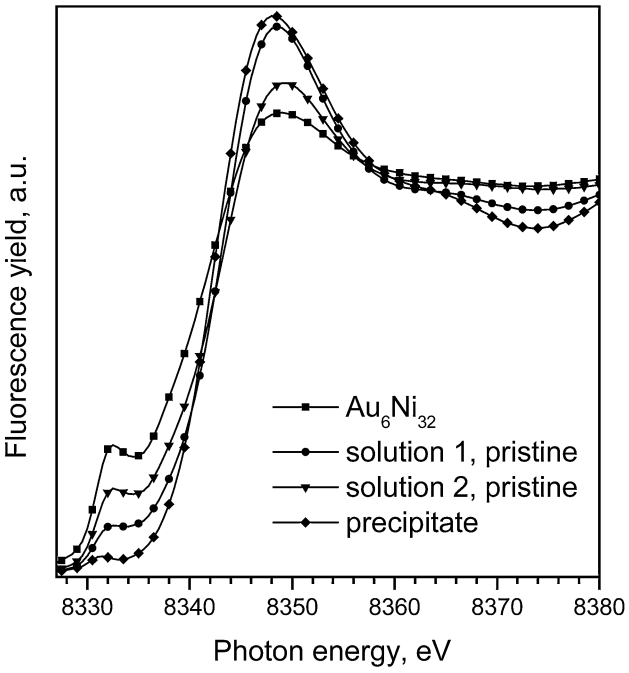

Fig. 4. Ni K-edge XANES spectra of the initial Au_6Ni_{32} cluster, pristine acetonitrile solutions **1** and **2**, and the precipitate.

paths has to be taken into account. Qualitatively, both pristine solutions show some differences in the shape of the first peak in Ni K-edge FT pattern as compared to that of the initial Au_6Ni_{32} cluster assuming a partial replacement of carbonyl ligands by oxygen species at Ni atoms. On the other hand, the two Au L_{III}-edge FTs of the solutions closely resemble that of Au_6Ni_{32} indicating that the Au_6 octahedron remains intact upon dissolution. Upon exposure to air for several hours, both solutions do not show any prominent changes as evidenced by time-resolved EXAFS and XANES series at Ni K- and Au L_{III}-edges (as a typical example, FTs for the solution **2** after 7–9 hours of air exposure are shown in Figs. 2 and 3). The changes, if any, can be reduced to an increase in the fraction of the unreacted Au_6Ni_{32} cluster. The most probable reason of that is a very slow oxidation of Au_6Ni_{32} in small amounts of MeCN solution by air (possibly, due to a formation of a thin film of oxidation products at a surface, which prevents further air access). Therefore, all the initial oxidation of the solutions **1** and **2**, most probably, takes place in a dissolution step, and thus the state of pristine solutions depend largely upon the preparation details, such as solvent pre-treatment. During air exposure, a slow precipitation withdraws insoluble oxidation products from the monitored area of the solution. In contrast, addition of Me_3NO causes immediate oxidation and precipitation of Au/Ni nanoparticles.

4. Summary and outlook

- An analysis of Ni K- and Au L_{III}-EXAFS spectra for the initial cluster compound $[Au_6Ni_{32}(CO)_{44}]^{6-}\cdot 6PPh_4\cdot 4.5CH_3CN$ yields values of structural parameters in a reasonable agreement with crystallographic data despite the heavy static disorder of the cluster core, which demonstrates applicability of EXAFS to similar high-nuclearity stoichiometric cluster compounds (see also [7, 8]).
- The oxidation product precipitated from the acetonitrile solution of the initial compound by Me_3NO was identified as a nanostructured material containing a core of Au atoms covered with a nickel oxide shell.

- Without addition of Me_3NO, the air oxidation of the acetonitrile solutions goes very slowly. A partial oxidation, most probably, occurs upon the preparation or ultrasonication of the solutions.
- In order to achieve a controlled oxidation of the initial cluster in a solution, chemical conditions of the reaction have to be adjusted (selection of protonic-aprotonic solvents mixtures, air blowing, or utilization of other mild oxidation promoters).
- Supplementary physical methods like XRD, IR, and HRTEM will be applied to verify the suggested structure of the final oxidation product.

Acknowledgements

Authors are indebted to Professor Lawrence F. Dahl (University of Wisconsin-Madison) who has kindly provided us with the initial Au_6Ni_{32} cluster and inspired this study. We are also grateful to Professor Edward Stern and Professor John Rehr (University of Washington, Seattle) for the UWXAFS and FEFF software, respectively. Authors also thank the KEK administration for the beamtime allocation and assistance in data collection. This work was supported by the Russian Foundation for Basic Research (grant #02-03-33225).

References

1. Schmid, G., Chem. Rev. **92**, 1709 (1992).
2. Guczi, L. *et al*., Top. Catal. **19**, 157 (2002).
3. Longoni, G. and Iapalucci, M. C. in "Clusters and Colloids. From Theory to Applications", (ed. by G. Schmid), (VCH, Weinheim, 1994), p. 91.
4. Vogel, W. *et al*., J. Phys. Chem. **101**, 11029 (1997).
5. Tran, N. T. *et al*., J. Am. Chem. Soc. **121**, 5945 (1999).
6. Moiseev, I. I. and Vargaftic, M. N. in "Catalysis by Di- and Polynuclear Metal Cluster Complexes", (ed. by R. D. Adams and F. A. Cotton), (Wiley-VCH, New York, 1998), p. 395.
7. Slovokhotov, Yu. L. in "Solid State Organometallic Chemistry: Methods and Applications", (ed. M. Gielen, R. Willem and B. Wrackmeyer), (Wiley, Chichester, 1999), p. 113.
8. Belyakova, O. A. *et al*., Book of abstracts, XAFS 11 conference (Ako, Japan, August 2000), P3-084, p. 274.
9. Shen, J.-K. *et al*., J. Am. Chem. Soc. **110**, 2414 (1988).
10. Newville, M. *et al*., Physica B **208&209**, 154 (1995).
11. Zabinsky, S. I. *et al*., Phys. Rev. B **52**, 2995 (1995).
12. Sasaki, S., Fujino, K. and Takeuchi, Y., Proc. Jap. Acad. **55**, 43 (1979)
13. Benfield, R. E. *et al*., J. Phys. Chem. B **105**, 1961 (2001).
14. Teo, B. K., Shi, X. and Zhang, H., J. Am. Chem. Soc. **114**, 2743 (1992).

